

Geochemistry of Late Archaean shaly BIF formed by oxic exogenic processes: an example from Ramagiri schist belt, Dharwar Craton, India

Meenal Mishra¹ 

Received: 2 January 2014 / Revised: 22 April 2014 / Accepted: 6 May 2014 / Published online: 18 June 2015
© Science Press, Institute of Geochemistry, CAS and Springer-Verlag Berlin Heidelberg 2015

Abstract The central block of the auriferous Ramagiri schist belt, in the Eastern Dharwar Craton, India consists of bimodal volcanics (mafic-felsic), shaly BIF and metasedimentary rocks. Geochemical studies of the associated shaly BIF have indicated the enrichment of the major and trace elements such as SiO₂, Al₂O₃, TiO₂, K₂O, MgO, Fe₂O₃(T), Zr, Y, Cr, Ni, alkali and alkaline earth elements indicates that the clastic component of the shaly BIF had their contribution from the contemporaneous bimodal volcanics. The concave chondrite normalized REE patterns share ubiquitously anomalous positive cerium anomaly, absence of positive europium anomaly and the overall HREE enrichment. The REE patterns resemble those from the modern day sea water, except for positive Ce anomaly. The data suggests that arc related bimodal volcanism had been the plausible source of Fe, silica, REE and other trace elements. The coherent behaviour of Fe, Ti, Mn and P with the REEs indicates that they got incorporated from Fe-Ti-Mn bearing primary minerals and secondary products like clays. The variability of REE patterns in the BIF formation samples probably results from the differences in scavenging efficiency. The BIF bears signatures of mixing of the contemporaneous clastic and chemical processes, as well as the changes accompanying diagenesis and metamorphism. The precipitation of Fe did not stop during the sedimentation in an island arc related tectonic setting. The BIF strongly lacks the signatures from hydrothermal input. The presence of positive cerium anomalies and the absence of

positive europium anomalies in the shaly banded iron formations imply that iron oxidation during BIF deposition took place in shallow waters rather than at depth, at oxic-anoxic boundary.

Keywords REE geochemistry · Cerium anomaly · Shaly BIF · Ramagiri schist belt · Eastern Dharwar Craton

1 Introduction

The geochemical features of the chemical sediments such as iron formations provide a useful insight into the chemistry of ancient sea water and exogenic processes. Banded Iron Formation of several basins have been studied world wide in detail for more than past two decades by numerous (Fryer 1977, 1983; Fryer et al. 1979; Condie 1981; Tren dall and Morris 1983; Miller and O’Nions 1985; Jacobsen and Pimental-Klose 1988; Derry and Jacobsen 1990; Shimizu et al. 1990; Towe 1991; Danielson et al. 1992; Bau and Dulski 1996; Bau 1993; Klein and Beukes 1993; Bau and Moller 1993; Klein and Ladeira 2000, 2002; Rosing and Frei 2004). The genetic models range from exhalative (Gross 1980, 1991; Goodwin et al. 1985, Goodwin 1991), evaporative (Eugester and Chou 1973; Garrels et al. 1973), biologically mediated precipitation (Cloud 1973; LaBerge 1988; Nealson and Myers 1990; Takahashi et al. 2007) and ocean upwelling (Holland 1973; Drever 1974). Fryer et al. (1979) and Fryer (1977, 1983) based on the presence of positive anomaly in Archaean BIF’s suggested that the characteristic REE concentrations by hydrothermal input.

The geochemical and genetic aspects of Banded Iron Formation from India have been addressed by Majumder et al. (1984), Chakraborty and Majumder (1986), Devraj and Laajoki (1986), Khan et al. (1992), Rao (1992), Arora

✉ Meenal Mishra
meenalmishra@ignou.ac.in

¹ School of Sciences, Indira Gandhi National Open University, New Delhi 110068, India

and Naqvi (1993), Siddaiah et al. (1994), Rao et al. (1995), Manikyamba et al. (1993, 1997), Manikyamba and Naqvi (1995) and Khan and Naqvi (1996).

REEs show a very similar geochemical behaviour, although elements like Ce and Eu show potential variations as a function of redox potential found in natural sedimentary oceanic environments. The Ce anomaly is the enrichment or depletion of cerium relative to the measured neighbouring elements La and Nd. The use of the cerium anomaly was first proposed by Elderfield and Greaves (1982). Under the oxic conditions, cerium exhibits positive anomaly due to its oxidation from Ce(III) to the Ce(IV) state, this is exceedingly insoluble. Therefore this results in depletion of cerium (negative anomaly) in the seawater which when compared to oxic sediments show relative enrichment. Conversely, in anoxic seawater Ce-containing sediments are mobilized so that Ce is released into the water column resulting in a positive anomaly in seawater (De Baar et al. 1985, 1988; De Baar 1991; Sholkovitz 1988; Sholkovitz and Schneider 1991; Wilde et al. 1996). Therefore, in anoxic sediments the cerium is depleted and shows a negative anomaly. There is no general agreement as to the mechanism for Ce-depletion in seawater and enhancement in sediments. The researchers attribute this phenomenon to oxidation of Ce^{+3} to Ce^{+4} and incorporation into Fe–Ti–Mn oxyhydroxides as CeO_2 or uptake into Fe–Mn nodules (Piper 1974; Elderfield et al. 1981; German and Elderfield 1990; De Baar 1991; German et al. 1991). Others (Liu et al. 1988; Liu and Schmitt 1990) attribute the enhanced presence of Ce in sediments to precipitation of $\text{Ce}(\text{III})\text{PO}_4$ preferentially to $\text{Ce}(\text{OH})_4$. At $\text{pH} > 7.5$, $\text{Ce}(\text{OH})_4$ precipitates associating with Fe–Mn–Al–Ti oxyhydroxide coatings on carbonate minerals.

The present paper reports the results of field investigations and discusses the interesting aspects of REE geochemistry and the significance of the positive cerium anomaly, in particular of the shaly BIF associated with the Central block from the Ramagiri greenschist belt, Eastern Dharwar Craton, India (Fig. 1). The Central block of Ramagiri schist belt in the Eastern Dharwar Craton is dominated by shaly Banded Iron Formation (shaly BIF), as compared to “true cherty BIF”. Quite often for the geochemical studies “pure samples” made up only of chert and iron minerals are chosen and the associated “clastic” material which are regarded as “contaminants” are ignored. In fact these contaminants or clastics are the integral part of BIF. As compared to the pure chemical fraction of BIF, the clastics are an excellent recorder of the depositional environment and processes of these chemogenic sediments (Derry and Jacobsen 1990). The banded iron formation in the Ramagiri schist belt consists predominantly of the oxide and mixed oxide-silicate facies types.

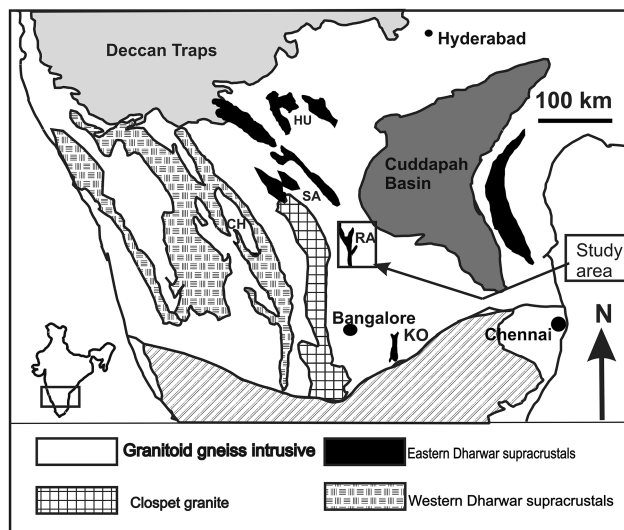


Fig. 1 Geological map of southern India. The Dharwar Craton is bounded by the Deccan Trap, Granulitic Terrane and Cuddapah Basin. Ra = Ramagiri (the study area shown in Fig. 2), Ko = Kolar, Sa = Sandur, Hu = Huttī, and Ch = Chitradurga schist belts. (after Chadwick et al. 1996). The block shows location of the Dharwar Craton. Inset shows the study area

2 Geological setting of Ramagiri Schist Belt

The Ramagiri Schist Belt in the Eastern Dharwar Craton is a N-S trending trident shaped, 2–3 km wide and 60 km long supracrustal belt, surrounded by granitoid gneisses and intrusive granites. The belt consists of Eastern, Central and Western arms that spread out northwards (Fig. 2). The Central arm of the belt has been divided into three distinct blocks (Eastern, Central and Western), based on lithological association, metamorphic grades, geochemical and isotopic characters of the metatholeiites (Zachariah et al. 1996, 1997). The detailed mapping of the Central block from the Central arm of the Ramagiri schist belt has been carried by Mishra and Rajamani (1999, 2003). The schist belt consists of dominantly bimodal volcanics (mafic-felsic volcanics) along with the subordinate metasedimentary rocks and minor chemogenic sediments. Pb–Pb isochron age obtained for the metabasalts of the central block of the central arm indicates that they are about 2750 Ma (Zachariah et al. 1995). U–Pb zircon age for the pyroclastics in the central block is about 2707 ± 18 Ma which has been considered as the time of emplacement of the felsic volcanics (Balakrishnan et al. 1999). The present study pertains to the geochemical studies of the shaly BIF from the Central block. Their impersistent lenticular nature points to an unstable environment for their deposition. The lithologies are highly disrupted along the tectonic contacts and crop out as lozenge shaped blocks. The various lithologies and the block itself are disposed subparallel to

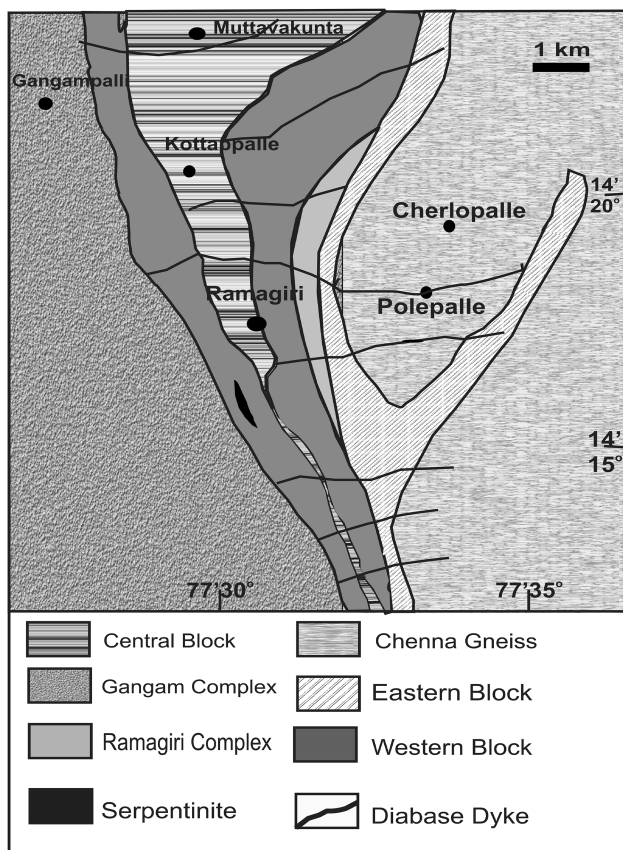


Fig. 2 Geological map of the trident Ramagiri schist belt, with three prongs pointing northward (after Zachariah et al. 1996). The Central and western prongs separate three granitoid terranes

the general schistosity and lack strike continuity—the features common in a tectonic melange ‘*sensu stricto*’. All the lithologies are strongly foliated with tapering ends and strike in a NNE–SSW direction. The contacts between the lithounits are broadly parallel to foliation planes ($N10^{\circ}$ E and $N10^{\circ}$ W) with steep to sub vertical ($>70^{\circ}$) dips. All the lithologies have undergone greenschist metamorphism with low fluid activity and intense deformation by repeated folding and shearing, but this is more conspicuously seen in the BIF units. The BIF are represented by rhythmic bands of iron and silica. BIF exhibit complex and intricate folding. Their thickened hinge areas are usually detached and are well preserved as hillocks in the Ramagiri schist belt (Fig. 3). The banded iron formation exhibit classical meso and microbanding. The strong lineations strictly parallel to the hinge are observed in all the folds. Folds are S, Z and M shaped. The limbs of the folds have been thinned out, boudinaged and displaced. The occurrence of several N-S trending, steeply dipping foliated iron bands within various units may be the result of tight isoclinal folding of high amplitude with steeply dipping plane suggesting complexity of folding. The



Fig. 3 Field photograph showing the detached hinge portion of the intricately folded banded iron formation. Circle shows a coin, as scale

plunge of the hinge is rarely gentle and ranges between 60° and 70° towards south. There are a set of boudin lines mostly parallel to the fold hinges and in some cases the boudins are rotated.

3 Petrography and mineralogy

The shaly banded iron formation of the Central block of Ramagiri schist belt is characterized by simple mineralogy. They exhibit penetrative deformation. They are composed of fine grained stretched clasts of quartz and feldspar in the matrix of muscovite, chlorite, sericite and minor opaques (Fig. 4a). However, alternate bands of finer and coarser materials consist of quartz, feldspar, muscovite and chlorite. The thin sections of the BIF show the microbands of quartz and iron oxide minerals. The meso and micro bands of cherty BIF are made up mainly of FeO oxides, micro-crystalline chert/quartz, with fair amount of chlorite. Magnetite with cubic to octahedral habit is the dominant iron oxide in shaly BIF (Fig. 4b). Quartz, when forms pure quartz band (free from iron minerals in their interstices) seem to be well crystalline from medium to coarse grained. This variation in grain size could be attributed to metamorphic processes.

The X ray diffraction data reveals that they are mainly composed of quartz, K-feldspar, iron minerals, chlorite, muscovite, sericite and other clay minerals like chamosite and kaolinite in varying proportions. The essential iron minerals include hydroxide (goethite), ilmenite and magnetite.

4 Sampling and analytical techniques

This study presents the geochemical data from shaly banded iron formation and shales sampled from the Central block of the Central arm of Ramagiri schist belt (Fig. 2). Total 12 samples of shaly BIF and 9 samples of shales were

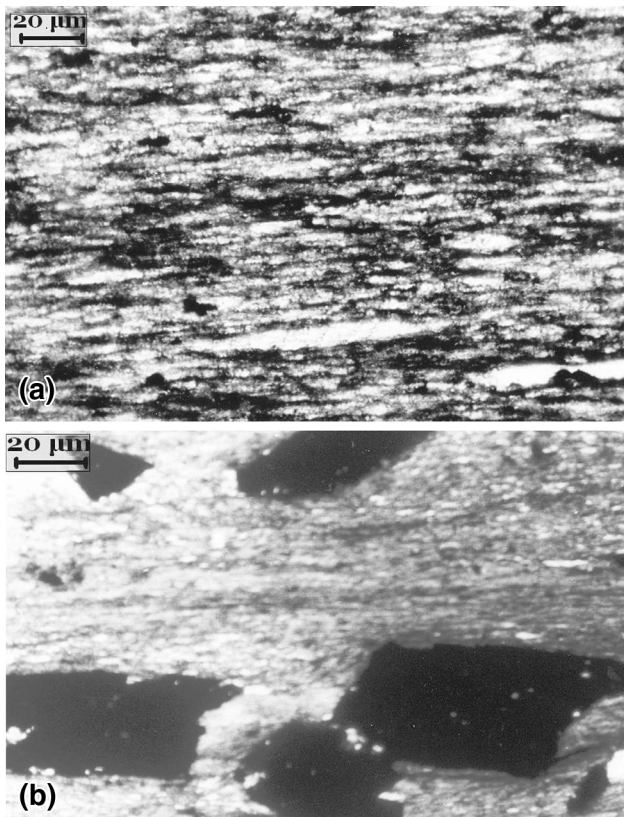


Fig. 4 **a** Photomicrograph of Shaly BIF showing stretched clasts of quartz and K Feldspar with dust of iron oxide. **b** Photomicrograph of Shaly BIF showing euhedral Magnetite

analyzed for major and trace and rare earth elements. Results of the analysis of shaly BIF and shale are presented in Tables 1, 2 and 3 respectively. Analytical details for REE determination are given in Giritharan and Rajamani (1998). Aliquots of homogenized rock powders were analyzed for major, trace and REE using a LABTAM 8440 ICP-AES at Jawaharlal Nehru University, New Delhi. REE were determined simultaneously by the polychromator in the LABTAM 8440 ICP-AES. Standardization for majority of major and trace elements excluding REE were based on USGS rock standards STM-1, RGM-1, W-2 and DNC-1 and in-house rock standards. Multi-elemental standards, prepared from pure REE metal standards (Johnson Matthey, USA) were used for instrument calibration. The efficacy of the sample dissolution procedures was checked by analyzing different aliquots of the same sample wherever possible. Among the trace elements, Zr was determined by LiBO₂ fusion method and analyzed by ICP-AES. SiO₂ was determined following a modified method of Shapiro and Brannock (1962) using a Spectronic-20 Bausch and Lomb Spectrophotometer. The analysis for Na₂O and K₂O was carried by Flame Photometer CHEMITO 1020, using solution ‘B’. The precision and accuracy of the analysis

are at the error level of <5 % for major and <10 % for trace elements. The reproducibility of REE data for RSB/37 and RSB/25 samples and the values of in-house standards, 90–57 and VM-9 indicate that the cerium positive anomaly in samples is not an analytical artifact. XRD data was obtained from Philips X'pert powder diffractometer and the minerals were identified using Philips X'pert HighScore (version 1) software program at JNU, New Delhi.

5 Geochemistry

5.1 Major elements

Among the major elements alumina and Fe₂O₃ (T) % has been used to distinguish between shaly BIF and shale. The shaly BIF shows ≥5 % Al₂O₃ and >10 % Fe₂O₃(T) whereas shale contains ≤10 % Fe₂O₃(T). There is large scale variation in the abundances of the major oxides (wt%) like SiO₂ (39.5–67.4), TiO₂(0.7–1.8), Al₂O₃(5.1–23.4), K₂O (0.8–3.9) and Fe₂O₃(T)(11.7–46.1). Harker variation plot for different elements are shown in Fig. 5a–i. Silica exhibits a sympathetic relation with alumina ($r = +0.7$) and titanium ($r = +0.6$), (Fig. 5a, b). The correlation matrices for elements measured in shaly BIF are presented in Table 4. Generally the shaly BIF samples show a scatter and a general decrease in Fe content with an increase in silica % ($r = -0.7$). This becomes more evident in Fe₂O₃ (T) and ΣREE relationship ($r = -0.24$), (Fig. 5c). Whereas, on the contrary silica shows a strong covariation with ΣREE ($r = +0.78$). Thus the geochemical signatures reflect that the REE budget for the shaly BIF seems to be mainly derived from silicate rich sources apart from their contribution from chemogenic sources. Majority of the samples show direct correlation of TiO₂ % with Al₂O₃ ($r = +0.81$), (Fig. 5d). The chemogenic sediments (shaly BIF) from Ramagiri schist belt exhibit an elevated Al₂O₃ and TiO₂ wt%, thus reflecting the incorporation of the clastic components (Ewers and Morris 1981). The scatter in TiO₂ and Al₂O₃ versus silica concentration is due to varying percentages of the clastic input in the different layers and levels from varying types of source rocks. MgO correlates strongly with CaO ($r = +0.54$), (Fig. 5i). However, MgO and CaO are fairly abundant but show much scatter (Fig. 4e) with respect to Fe₂O₃(T) due to presence of secondary minerals like clays and chemogenic input, in addition to mafic component from the clastics. This aspect becomes clear from the Fe₂O₃(T) and MgO ($r = 0.2$), relationship, which is not at all defined. MgO in the Ramagiri shaly BIF ranges between 0.3 and 4.8 %, quite similar to the modern ferro-oxyhydroxides from East Pacific Rise (1–3 %; Marchig et al. 1982). MnO is less in abundance as compared to P₂O₅,

Table 1 Major and trace element data for shaly BIF from Central block of Ramagiri schist belt, Andhra Pradesh district

Samples	RSB/83	RSB/21	RSB/99	RSB/100	RSB/37	RSB/20	RSB/25	RSB/75	RSB/16	RSB/102	RSB/58	RSB/27	Av. RSB shale	
Major oxides (%)														
SiO ₂	39.4	39.5	45.3	45.2	48.4	49.0	49.3	50.7	52.2	55.2	66.9	67.4	59.7	
TiO ₂	1.05	0.56	0.9	0.7	1.34	1.38	1.29	1.11	1.56	1.81	1.24	1.3	1.26	
Al ₂ O ₃	12.5	5.9	5.3	5.1	21.2	15.3	23.4	16.6	18.2	12.3	13.9	12.1	14.2	
Fe ₂ O ₃ (T)	32.5	40.7	45.2	46.1	14.2	27.0	14.3	19.4	13.1	23.5	11.7	12.5	9.4	
MnO	0.020	0.030	0.010	0.030	0.040	0.020	0.030	0.040	0.060	0.020	0.030	0.040	0.050	
MgO	3.0	3.8	0.5	0.4	4.8	2.6	1.4	3.9	3.6	3.9	0.7	0.7	1.5	
CaO	0.3	0.2	0.1	0.04	0.5	0.3	0.4	0.3	0.7	0.2	0.2	0.3	0.4	
Na ₂ O	0.01	0.01	bdl	bdl	1.2	bdl	0.7	0.02	1.3	0.02	bdl	bdl	0.5	
K ₂ O	1.10	0.8	0.9	0.9	3.9	1.2	3.7	2.1	3.1	2.30	2.3	2.6	3.5	
P ₂ O ₅	0.3	0.8	0.3	0.4	0.3	0.4	0.4	0.4	0.7	0.5	0.5	0.4	bdl	
TOTAL	90.1	92.3	98.4	98.9	95.9	97.3	94.9	94.6	94.5	99.7	97.4	97.3	90.5	
Ti/Al	10.12	8.95	5.00	6.19	13.44	9.39	15.41	12.73	9.92	5.76	9.52	7.91	9.58	
Trace elements (ppm)														
Ba	148	148	155	147	513	151	505	275	496	172	105	110	582	
Sr	60	22	15	8	70	16	72	32	65	17	16	20	109	
Cr	306	205	107	185	250	150	266	337	231	265	107	120	217	
Ni	169	138	145	124	110	138	116	164	121	277	158	170	165	
Zr	119	185	119	185	224	140	224	120	246	106	143	135	186	
Y	17	14	18	20	20	18	21	19	21	12	14	17	20	
Co	44	51	45	46	55	42	48	49	46	43	46	47	—	
Cu	160	119	144	138	141	117	143	162	142	146	126	125	—	
Ni + Co + Cu	124	103	111	103	102	99	102	125	103	155	110	114	—	
Zr/Y	7.0	13.2	6.6	9.3	11.2	7.8	10.7	6.3	11.7	8.8	10.2	7.9	9.3	

Table 2 REE data for shaly BIF from the Central block of Ramagiri schist belt, Andhra Pradesh district

Samples	RSB/83	RSB/21	RSB/99	RSB/100	RSB/37	RSB/20	RSB/25	RSB/75	RSB/16	RSB/102	RSB/58	RSB/27	Av. RSB shale
REE (ppm)													
La	5.8	4.6	4.8	4.9	4.8	6.2	3.9	10.1	9.9	9.0	8.9	9.0	21.5
Ce	27.8	26.5	24.9	25.0	17.2	28.1	16.4	30.2	29.5	28.1	28.6	29.0	39.8
Nd	7.8	5.6	5.7	5.7	4.4	8.1	4.3	7.9	7	7.5	8.3	7.9	17.4
Sm	1.8	1.3	1.1	1.0	1.6	2.1	1.6	1.6	1.5	2.0	3.0	3.4	3.5
Eu	0.57	0.25	0.27	0.26	0.6	0.6	0.58	0.797	0.78	0.64	0.97	1.01	1.03
Gd	1.7	0.7	0.7	0.8	2.0	2.0	2.2	2.7	2.5	2.3	2.8	2.8	3.3
Dy	1.9	0.8	0.9	0.9	2.9	2.2	3.0	3.4	3.3	3.1	3.9	3.9	2.9
Er	1.3	0.5	0.5	0.5	2.2	1.6	2.3	2.3	2.2	2.5	2.0	2.1	1.9
Yb	1.41	0.69	0.7	0.68	2.27	1.04	2.38	2.29	2.2	2.69	2.05	2.09	1.77
Σ REE	50.1	40.94	39.6	39.7	38.0	51.9	36.6	66.2	58.88	61.8	66.3	67.5	66.3
Σ LREE	43.8	38.3	36.7	36.8	28.6	45.1	26.8	50.6	48.7	47.2	49.7	50.3	—
Σ HREE	6.3	2.7	2.9	2.9	9.4	6.8	9.9	10.7	10.2	10.5	10.8	10.9	—
[La/Yb] _{SN}	0.28	0.46	0.47	0.49	0.14	0.41	0.11	0.30	0.31	0.23	0.30	0.29	—
[Nd/Yb] _{SN}	0.49	0.71	0.71	0.74	0.17	0.69	0.16	0.30	0.28	0.24	0.36	0.33	—
[Gd/Yb] _{SN}	0.64	0.54	0.53	0.63	0.48	1.04	0.50	0.63	0.61	0.46	0.73	0.72	—
[La/Yb] _N	2.73	4.40	4.54	4.74	1.38	3.94	1.09	2.92	2.97	2.20	2.86	2.85	—
[Nd/Yb] _N	2.83	1.94	2.84	2.94	2.72	0.97	0.68	0.63	1.20	1.11	1.32	1.41	—
[Gd/Yb] _N	0.97	0.81	0.80	0.94	0.71	1.56	0.75	0.95	0.91	0.69	1.09	1.09	—
[Ce/Ce]*	1.3	1.0	1.0	1.0	1.0	1.4	0.8	2.2	1.9	2.0	2.0	2.2	—

which is ranges between 0.4 and 0.8 %, both of them show a positive correlation to each other.

The positive correlation of alkali oxides (K_2O and Na_2O) and Al_2O_3 ($r = +0.68$ and $+0.86$) indicates lots of clastic input of minerals like feldspars. This direct variation suggests their clastic input from within basin felsic volcanic source. The presence of high K_2O (1–4 %) and alumina content (16–23 %) in some of the shaly BIF samples can also possibly be attributed to the precipitation of celadonite clay from the sea water (a type of illitic clay, Fe rich K mica) associated with the submarine alteration of primary volcanic material (Tlig and Steinberg 1982). This can also be corroborated with XRD data which indicates the presence kaolinitic clay. On the contrary the positive relationship between pair of elements like MgO – TiO_2 ($r = +0.54$), CaO – TiO_2 ($r = +0.5$), MgO – Al_2O_3 ($r = +0.52$), CaO – MgO ($r = +0.54$) and TiO_2 – K_2O ($r = +0.6$) signifies that the sediments in the BIF were derived from the mafic source. While the direct correlation between SiO_2 – Al_2O_3 ($r = +0.72$), SiO_2 – Al_2O_3 ($r = +0.72$), SiO_2 – TiO_2 ($r = +0.8$), Al_2O_3 – K_2O ($r = +0.89$) and CaO – K_2O ($r = +0.71$) points towards the felsic contribution.

5.2 Trace elements

Among the trace elements Ba exhibits a strong positive correlation with Sr ($r = +0.80$) whereas Zr shows direct variation with Ba ($r = +0.53$) and Sr ($r = +0.34$). SiO_2

($r = +0.6$), TiO_2 ($r = +0.55$) and Al_2O_3 ($r = +0.62$) exhibit a well defined relationship to Zr (Fig. 6). This sympathetic behaviour shown by above three oxides and Zr provides an important clue for Σ REE budget for BIF. HREE's seem to be hosted in mineral like zircon ($r = +0.4$). This is also favoured by P_2O_5 –Zr relationship ($r = +0.42$) which also covaries in a fairly coherent manner (Clarke Anderson 1984). Ba also reveals a direct relationship to majority of major oxides like Al_2O_3 ($r = +0.78$, Fig. 4g), CaO ($r = +0.78$), K_2O ($r = +0.8$). Whereas Sr covaries directly with Al_2O_3 ($r = 0.76$, Fig. 4e), CaO ($r = +0.78$) and K_2O ($r = +0.67$). A strong affinity between K_2O –Ba and Al_2O_3 – K_2O –Ba–Sr can be attributed to presence of micas and feldspars respectively in their mineralogy. Ni abundances vary between 110 and 227 ppm and of Zr vary from 37 to 246 ppm. Ni/Zr ratios ($r = +0.4$) and their behaviour demonstrate the clastic contribution to these rocks. Cr content of shaly BIF show a positive correlation with Ni ($r = +0.6$) and MgO ($r = +0.76$) (Fig. 5j, k) indicating the contribution from a mafic source. However the ferruginous sediments formed by chemical precipitation from normal seawater do not have such high concentrations of these elements. Therefore, higher abundances of these elements indicate that enrichment in Cr and Ni contents is due to the terrigenous input. The Zr and Cr (107–337 ppm) relationship ($r = +0.59$) brings out this aspect more clearly. The

Table 3 Geochemical data for Shales from the Central block of Ramagiri schist belt

Samples	M-1	M-2	M-3	M-4	M-5	M-6	M-7	M-8	M-9
Major oxides (%)									
SiO ₂	58.6	59.1	59.7	60.0	60.5	61.0	61.4	73.6	74.5
TiO ₂	1.27	1.11	1.26	1.13	1.31	0.77	1.2	0.24	0.37
Al ₂ O ₃	19.3	17.1	16.4	17.1	18.01	18.2	15.5	8.5	15.5
Fe ₂ O ₃ (T)	9.8	6.9	7.9	9.4	9.5	6.9	8.3	8.6	0.9
MnO	0.03	0.08	0.08	0.04	0.07	0.04	0.07	0.05	0.02
MgO	2.2	2.2	2.5	1.5	2.5	1.4	3.1	3.5	0.2
CaO	0.2	0.7	1.5	0.4	1.5	1.1	1.2	0.7	0.2
Na ₂ O	1.1	1.4	1.8	0.5	1.7	2.5	1.3	0.4	1.8
K ₂ O	2.5	1.6	2	4.9	2.1	2.1	1.5	0.7	2.3
P ₂ O ₅	0.1	0.08	0.06	0.09	0.1	0.1	0.09	0.1	0.02
TOTAL	95.1	90.2	94.1	95.0	97.2	94.1	93.7	96.3	95.7
Trace elements (ppm)									
Ba	344	324	552	582	557	235	408	11	516
Sr	183	182	164	109	223	239	201	16	532
Cr	292	239	275	217	281	269	252	83	222
Ni	112	82	93	65	77	95	97	61	122
Zr	150	178	164	186	167	204	195	62	141
Y	19	20	20	18	21	21	21	9	23
La	18.2	36.4	38.1	45.2	40.1	17.9	35.6	25.1	8.8
Ce	40.7	79.8	79.9	94.6	84.7	39.8	78.4	51.8	86.5
Nd	19.5	35.8	31.7	38.9	34.1	17.4	34.5	16.6	35.4
Sm	4.4	6.2	4.9	7.6	5.4	3.5	5.9	3.2	5.2
Eu	1.26	1.71	1.41	1.77	1.5	1.03	1.6	0.78	1.24
Gd	4.2	5.0	4.5	5.0	4.5	3.3	4.8	2.3	3.7
Dy	4.4	4.8	4.5	5.2	2.5	2.9	4.5	2.0	2.2
Er	2.6	3.1	2.9	3.0	1.8	1.9	2.8	1.5	1.6
Yb	2.58	2.54	2.51	2.3	1.2	1.77	2.3	1.30	1.00
ΣREE	79.5	139.0	132.3	158.3	135.7	71.6	134.8	79.5	136.7
[La/Yb] _N	234.8	390.6	374.5	449.3	376.9	2.6.2	376.8	226.9	271.0
[Gd/Yb] _N	1.3	1.6	1.4	1.7	3.0	1.5	1.7	1.4	3.0

relationship of Fe₂O₃ (T) with Ba, Sr, Cr, Ni, Y, Co and Cu (Table 1) seems to be erratic and poorly defined. This observation brings out more clearly the earlier inference that the Fe component in the BIF includes a major contribution from chemogenic sources, in addition to silicate rich sources. The overall enrichment of the major and trace elements such as SiO₂, Al₂O₃, TiO₂, K₂O, MgO, Fe₂O₃(T), Zr, Y, Cr, Ni, alkali and alkaline earth elements supports that the clastic component of the shaly BIF had their contribution from the bimodal (felsic-mafic) provenance though the input from terrigenous sources cannot be completely denied. The higher abundances of these elements in the chemogenic sediments can be attributed to volcanioclastic contribution resulting from the contemporaneous bimodal volcanism in an island arc setting (Mishra and Rajamani 1999, 2003). Alternatively, high Mg, Ni and Cr flux in the chemogenic sediments can be credited to Mg

rich composition of Archean crust (McLennan 1989; Taylor and McLennan 1985). Therefore continental contribution cannot be completely ruled out.

5.3 REE geochemistry

The shale normalised patterns of the shaly iron formation from Ramagiri schist belt (Fig. 7) share important features e.g., ubiquitously strong positive cerium anomaly in all the samples, a slight positive Eu anomaly in some of the samples, HREE enrichment and [Gd/Yb]_{SN} < 1 shale. The presence of positive Ce anomaly is one of the outstanding and interesting aspect of shaly BIF, therefore [Nd/Yb]_{SN} ratios ~ 0.16–0.74, are used instead of [La/Yb]_{SN} to get an idea of REE fractionation. Large variations are noticed in [Nd/Yb]_{SN} ratios ~ 0.1–0.7. The direct relationship between ΣREE and SiO₂ ($r = +0.78$), Al₂O₃ ($r = +0.8$)

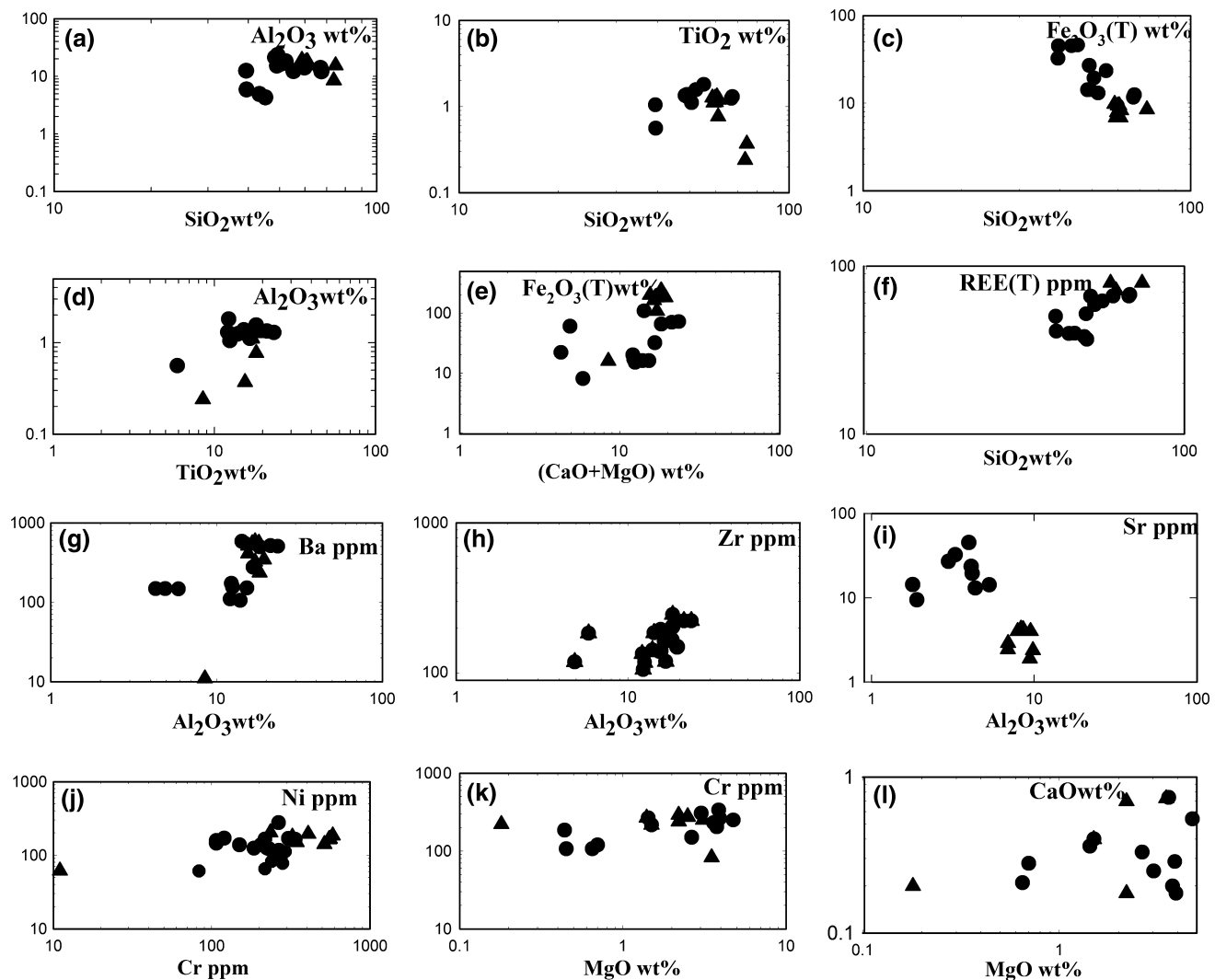


Fig. 5 Harker variation diagram showing trends of different major, trace elements and Σ REE. Closed circle- shaly BIF; closed triangle-shale

and TiO_2 ($r = +0.46$), K_2O ($r = +0.44$) and Zr ($r = +0.60$) is very convincing in demonstrating that increases in Σ REE are the consequence of simultaneous clastic deposition (Fig. 6). Σ REE content of Al_2O_3 rich shaly BIF is significantly higher than those with low Al_2O_3 . The shale normalized average REE values for the contemporaneous shales from Ramagiri schist belt (Av. RSB Shale) (Table 3) have been plotted which shows a completely flat pattern (Fig. 7). BIF samples are normalized with Average Archaean Shales (Condé 1993). The shale normalized REE patterns of shaly BIF are depleted in LREE's in comparison to the HREE. The REE patterns (Fig. 7) show that the depleted LREE concentration is even lower than the shale (which is less than 1). Whereas HREE are enriched with abundances equal to shale normalized values. The flat pattern of shale is suggestive of terrigenous source which can be corroborated by the enrichment of

both major and trace elements. Among the REE group, the HREE show a stronger positive correlation with terrigenous elements like Si, Al, Ti, Mn, Mg, K, P, Ni and Zr compared to middle REE (MREE) and light REE (LREE). Between the LREE and HREE, the terrigenous contribution is richer in the HREE than the LREE. However, the HREE enrichment and $[Nd/Yb]_{SN} \leq 0.5$ are the features which are characteristic of modern sea water (Elderfield and Greaves 1982; De Baar et al. 1985; Goldstein and Jacobsen 1988). Derry and Jacobsen (1990) have found a similarity in overall shape of the REE patterns of Archaean oxide facies BIF and modern sea water, except for the strong positive cerium anomaly and a slight positive europium anomaly. The enrichment of the HREE over REE in the shale normalized patterns has been described by Byrne and Kim (1990) as the result of increased stability of complexes with hydroxyl, carbonate and phosphate.

Table 4 Correlation matrix for the elements measured in Shaly BIF from Ramagiri schist belt, Andhra Pradesh, India

	SiO ₂	TiO ₂	Al ₂ O ₃	FeO(T)	K ₂ O	P ₂ O ₅	Ba	Sr	Cr	Ni	Zr	Y	Co	Cu	Ce/Ce*	ΣREE	ΣLREE	ΣHREE
SiO ₂	1.00																	
TiO ₂	0.60	1.00																
Al ₂ O ₃	0.70	0.80	1.00															
FeO(T)	-0.69	-0.72	-0.83	1.00														
K ₂ O	0.44	0.64	0.86	-0.86	1.00													
P ₂ O ₅	0.01	0.03	-0.11	-0.07	0.03	1.00												
Ba	-0.13	0.35	0.78	-0.49	0.79	0.04	1.00											
Sr	-0.24	0.28	0.76	0.50	0.67	-0.05	0.85	1.00										
Cr	-0.43	0.16	0.44	-0.15	0.26	0.02	0.47	0.58	1.00									
Ni	0.28	0.45	-0.21	-0.03	-0.13	0.03	-0.45	-0.38	0.60	1.00								
Zr	0.60	0.55	0.62	-0.83	0.81	0.42	0.53	0.34	0.50	0.40	1.00							
Y	-0.23	-0.07	0.44	-0.11	0.35	-0.33	0.67	0.55	0.19	-0.75	0.00	1.00						
Co	-0.12	-0.27	0.28	-0.21	0.45	0.10	0.51	0.42	0.23	-0.47	0.42	0.26	1.00					
Cu	-0.29	0.12	0.22	-0.01	0.14	-0.40	0.30	0.43	0.74	0.20	-0.03	0.27	0.01	1.00				
Ce/Ce*	0.73	0.51	0.10	-0.53	0.11	0.22	-0.31	-0.27	-0.03	0.54	0.44	-0.38	-0.33	0.03	1.00			
ΣREE	0.78	0.46	-0.17	-0.24	-0.22	0.26	-0.49	-0.42	-0.10	0.51	0.17	-0.41	-0.49	-0.02	0.93	1.00		
ΣLREE	0.72	0.80	0.75	-0.95	0.78	-0.01	0.38	0.35	0.26	0.28	0.81	0.00	0.06	0.18	0.67	0.37	1.00	
ΣHREE	0.77	0.76	0.60	-0.53	0.16	0.19	-0.23	-0.24	0.01	0.55	0.49	-0.32	-0.31	0.08	0.99	0.91	0.68	1.00

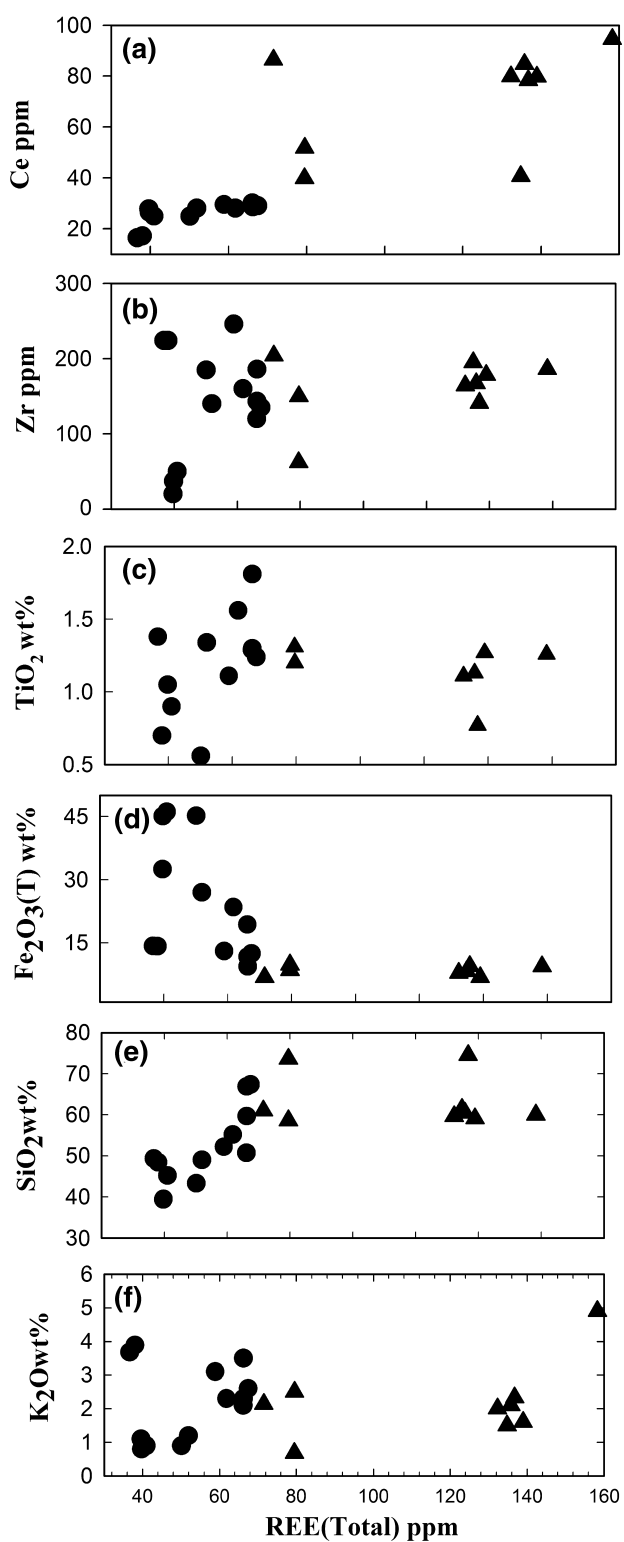


Fig. 6 Variation diagram showing trends of different major, trace elements using Σ REE as index of differentiation. Closed circle- shaly BIF; closed triangle-shale

The chondrite normalized patterns for shaly BIF show a considerable fractionation, with $[La/Yb]_N \sim 3$ and slight fractionation of HREE with $[Nd/Yb]_N \sim 1.71$ (Fig. 8). The

chondrite normalised REE patterns of shales (Table 3) from the Central block of Ramagiri schist belt resemble those of the shaly BIF, except for the absence of positive Ce anomaly and higher LREE abundances (Figs. 8, 9, 10, 11). The Av. RSB Shale resembles the typical Archaean shale (Taylor and McLennan 1985; McLennan 1989). The patterns for Av. RSB shale are highly fractionated with REE's average $[La/Yb]_N$ ratio = 300 and less fractionated HREE with $[Gd/Yb]_N = 1.8$. On their comparison, the chondrite normalized patterns also corroborate with the inference that the HREE of the shaly BIF seem to have been inherited from the contemporaneous RSB shales which were simultaneously depositing in an arc related basin. In general, all the REE patterns have concave patterns (LREE > MREE < HREE) (Fig. 8). All the samples show a strong Ce positive anomaly and the total REE content varies between 40 and 67. On average the Ce is 30 times and Yb is 10 times on the chondrite normalized diagram. On the basis of REE abundances and chondrite normalized patterns of shaly BIF, can be grouped into 3 different types (Fig. 9).

Group 1 It is represented by two samples (RSB/99 and RSB/100), with Σ REE = 40 and slight HREE enrichment ~ 36 . They have strong +ve Ce anomaly (0.9–1) and $[Nd/Yb]_N$ ratios = 13.1 and $Ce/Ce^* = 1$.

Group 2 This includes RSB/25 and RSB/37 (Fig. 9) which is characterised by Σ REE = 36–38, while the HREE are enriched with $[Nd/Yb]_N$ ratios = 18.4 and $Ce/Ce^* = 0.9$.

Group 3 This includes rest of the samples with Σ REE ranging between 50 and 67 (Fig. 9) and $[Nd/Yb]_N$ ratios = 27.5 and $Ce/Ce^* = 1.75$.

The enhanced cerium concentration shown by the absolute REE abundances of BIF behave coherently with Fe ($r = +0.69$), MnO ($r = +0.2$), P_2O_5 ($r = +0.33$), TiO_2 ($r = +0.7$), Σ REE ($r = +0.95$) and Σ LREE ($r = +0.99$), (Fig. 9). The geochemical signatures indicate that discrete Fe, Ti, Mn and P minerals played an important role in scavenging REE's, particularly cerium during the formation of Banded Iron Formation. It appears that REEs got incorporated with the Fe–Ti–Mn bearing primary minerals and secondary products like clays. Fe–Ti oxyhydroxides coating has been reported to be an important phase containing the REE's in sediments (Nesbitt 1979; Middelburg et al. 1988). The variability of REE patterns in the BIF formation samples probably results from the differences in scavenging efficiency. Cerium is influenced by the detrital/terrigenous input, depositional environment and interplay of these factors, may obscure original characteristics of the sediments (McLeod and Irving 1996). Dutta et al. (2005) found a positive correlation of REE with Fe content of the nodules of the Indian Ocean. The REE data of the metaliferous sediments from East Pacific Rise show evidence of

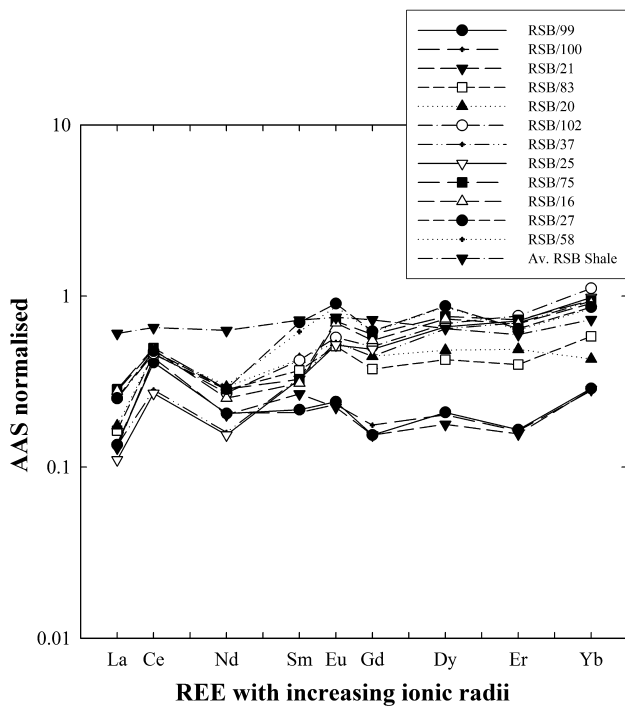


Fig. 7 Shale normalised REE abundances of the shaly BIF. The pattern for Av. RSB shale plotted for comparison. Value for average Archaean shale (AAS) is from (Condie 1993)

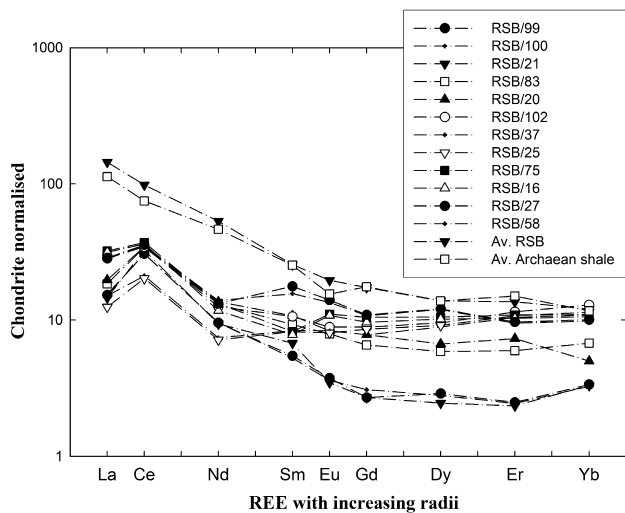


Fig. 8 Chondrite normalised REE patterns of shaly BIF and for comparison Av. RSB shale and Av. Archaean shale have been plotted. Chondrite values are from Sun and McDonough (1989)

REE scavenging by Fe-oxyhydroxide and a clear pattern of increasing LREE depletion with distance from ridge axis (Ruhlin and Owen 1986; Derry and Jacobsen 1990). The similarities between the REE patterns of modern metalliferous sediments and the oxide facies BIF's suggests that the scavenging by Fe hydroxides was the mechanism responsible for the incorporation of the REE's into BIF.

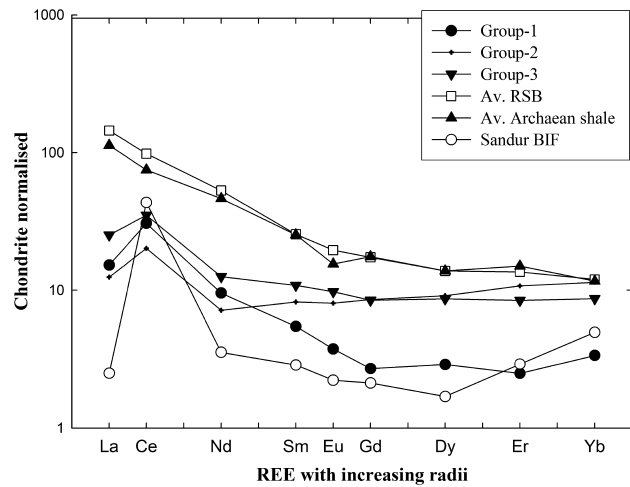


Fig. 9 Chondrite normalised average REE patterns for Groups-1, 2 and 3 of shaly BIF. For comparison Av. RSB shale and Av. Archaean shale have been plotted. REE patterns of the average of few samples from Sandur schist belt showing positive cerium anomaly have been plotted. Data taken from Manikyamba et al. (1993)

This is also evident from the presence of iron minerals in XRD data. The overall trend of REE's in BIF is compatible with the mechanism of oxide facies (Derry and Jacobsen 1990).

After normalization with AAS the LREE/HREE ratios in most of the samples are <1 and exhibit a simultaneous decrease of LREEs and increase of HREEs. Simultaneous enrichment in both LREE and HREE in the Shaly BIF appears to be the consequence of deposition of felsic and mafic clastic debris along with the chemical precipitates. Ce depletion in pure chemical precipitation and enrichment in BIF with clastic inputs suggests that Ce^{3+} was oxidized to Ce^{4+} , to be separated from the system of chemical precipitation and thereby accumulated in the clastic component. The data shows the clear signatures of REE concentrations of clastic input are superimposed by chemical flux. The REE abundances of the Av. RSB Shale have been explained by mixing model of the end members of Archean bimodal igneous suite of mafic and felsic volcanics in an island arc related basin (Mishra and Rajamani 1999, 2003). Figure 12 shows the comparison of the absolute REE patterns and abundances of average mafic, dacitic and rhyolitic volcanics with average RSB Shale from the Central block. After the correlation of the various geochemical data it is appears that the clastic deposition continued even during the times of precipitation of BIF. The precipitating chemogenic sediments were subsequently contaminated by the shaly contribution. Even minor amounts of extraneous clastic input in iron formation could drastically affect their REE contents and patterns (Fryer 1977, 1983). Sholkovitz (1988) has suggested that the terrigenous input of REE from the continent and authigenic

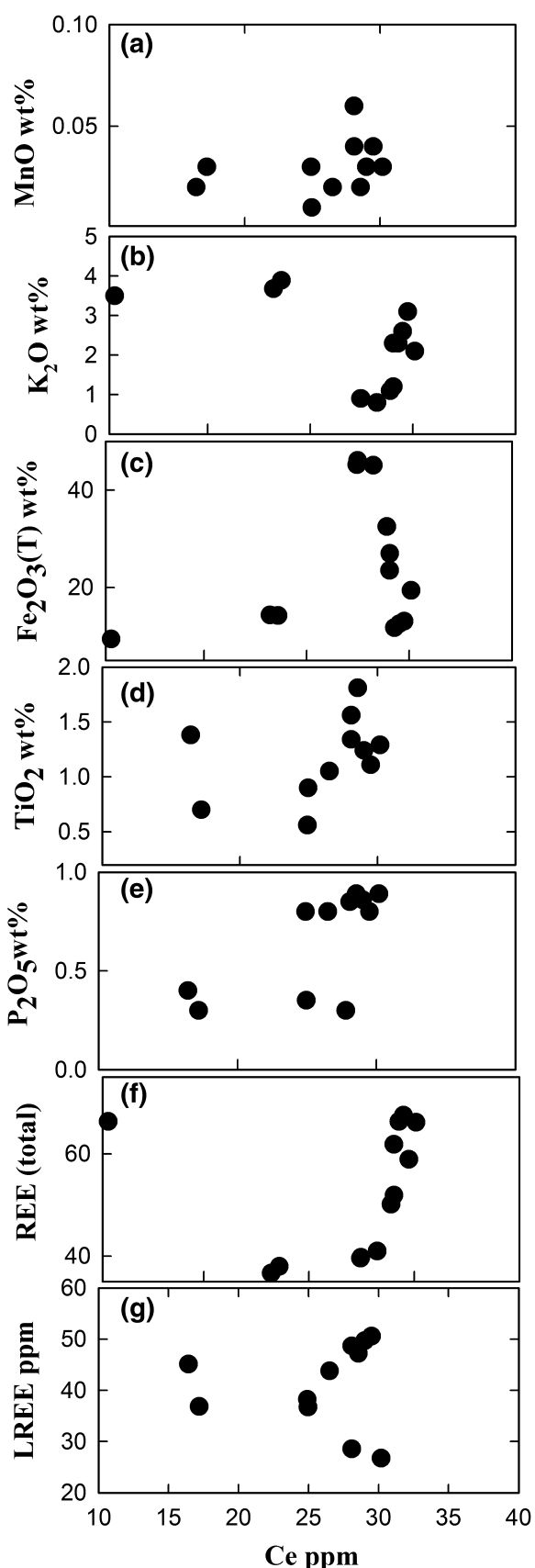


Fig. 10 Variation diagram showing trends of different major, trace elements using cerium concentration as index of differentiation

removal of REE from the water column and early diagenesis are major processes that control the enrichment and depletion of metals in sediments. Therefore the geochemical data suggests that the shaly BIF are the result of mixing of the 2 end members (Fig. 12) (a) precipitation of Fe and (b) the contribution of the clastics from contemporaneous mafic and felsic contribution.

6 Comparison with other BIF

Based on the available data Fryer (1977, 1983) and Fryer et al. (1979) inferred that significantly anomalous Ce abundances are not known from Archean iron formation, whereas in Proterozoic BIF's cerium is definitely anomalous with examples of both enrichment and depletion. However Dymek and Klein (1988) have reported that Archean sea water possessed a negative Ce anomaly much like present day sea water, and the process which scavenge Ce were already operative 3.8 Ga ago based on the studies on BIF from Greenland. Rosing and Frei (2004) have discussed the geochemical evidences for oxygen production in Early Archaean for >3.7 Ga old sediments from Isua supracrustal belt. This idea has been further supported by Knoll (2003) based on strong palaeobiological evidences. The BIF samples from 2.7 Ga Michipicoten (Goodwin et al. 1985; Goodwin 1991) and Bjornevann (Jacobsen and Pimental-Klose 1988) greenstone belts exhibit a large positive cerium anomaly, suggesting local redox cycling of Ce or possibly photooxidation of cerium during Archean. BIF with positive Ce anomaly have been reported from the Dharwar schist belts such as Kudremukh (Khan et al. 1992), Chitradurga (Rao and Naqvi 1995), Sandur (Manikyamba and Naqvi 1995; Manikyamba et al. 1993) and Bababudan (Arora and Naqvi 1993). Manikyamba et al. (1993) have reported similar REE abundances and patterns in the samples of BIF from Sandur schist belt with moderate to strong positive Ce anomalies. The REE data of the BIF from Sandur schist belt has been plotted with that from RSB, for comparison (Fig. 9). The data of BIF from Sandur schist belt has been taken from Manikyamba et al. (1993), Manikyamba and Naqvi (1995) and the data have been provided by C. Manikyamba on personal request. On the basis of positive cerium anomaly in the REE abundances, they have suggested that intermittently oxidizing environment prevailed during the Archean. Rao and Naqvi (1995) have also reported Ce enrichment relative to La in BIF from Chitradurga schist belt.

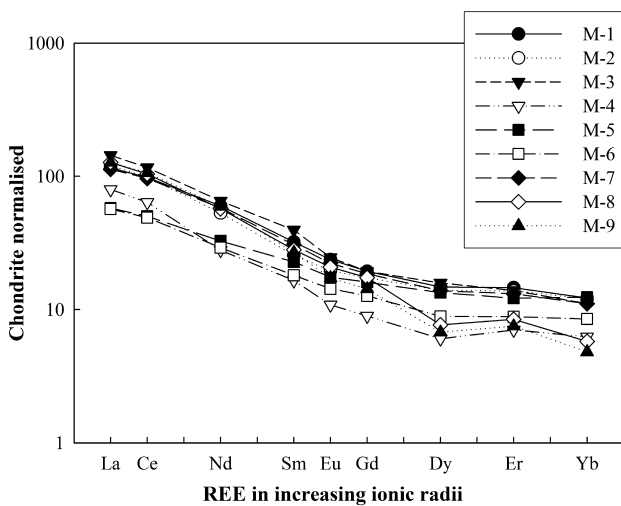


Fig. 11 Chondrite normalised REE patterns of the shales from the Central block of the Ramagiri schist belt

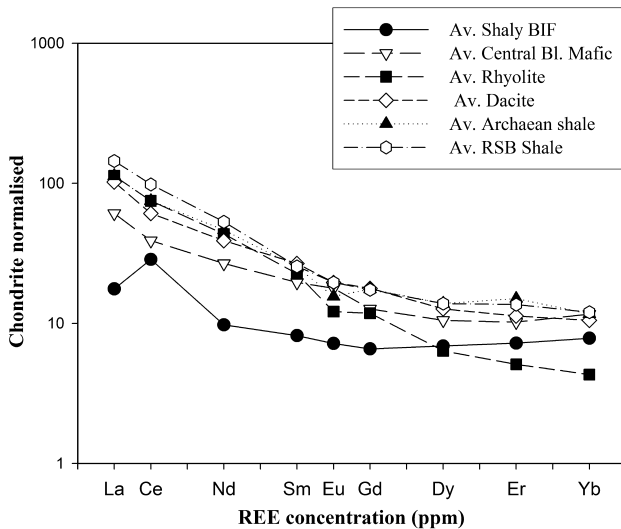


Fig. 12 Chondrite normalised REE patterns of the shaly BIF are compared with the average Ramagiri rhyolite, dacite, metatholeites and shales from the Central block from (Mishra and Rajamani 1999, 2003)

7 Discussion and conclusion

REE concentrations of the shaly BIF from Archaean Ramagiri schist belt show a great variation in elemental abundances. The shales from the Central Block of Ramagiri schist belt indicate a mixed provenance from both felsic and mafic volcanics (bimodal volcanics from Central Block) in an arc related basin (Mishra and Rajamani 2003). REE of shaly BIF exhibit concave patterns ($\text{LREE} > \text{MREE} < \text{HREE}$), a strong Ce positive anomaly, considerable REE fractionation, with $[\text{La/Yb}]_{\text{N}} \sim 3$ and slight fractionation of HREE with $[\text{Nd/Yb}]_{\text{N}} \sim 1.7$. Chondrite

normalised REE patterns of adjacent shales resemble those of the shaly BIF, except for the absence of positive Ce anomaly and higher LREE abundances. Thus the REE patterns of shaly BIF with the positive cerium anomaly represent the end product of a complex series of events that record the properties of the solutions that precipitated along with the clastic sediments.

The shaly BIF bears signatures of mixing of the contemporaneous clastic and chemical components, as well as the changes accompanying diagenesis and metamorphism. The chondrite normalized REE patterns obtained from the present day active hydrothermal settings reveal that such solutions are generally characterized by low REE, La enrichment, an exceptional prominent positive Eu anomalies with or without negative cerium anomaly (Fryer et al. 1979; Fryer 1977, 1983; Michard and Alberede 1986; Michard et al. 1993; Piedgras et al. 1979). The shaly BIF from the Central block of the Ramagiri schist belt are characterized by the enriched REE patterns with positive cerium anomaly and the absence of positive europium anomaly. These geochemical signatures suggest that the shaly BIF from Ramagiri lacks the hydrothermal input.

The overall REE patterns resemble those from the modern day sea water, which are exceptionally HREE enriched, except for positive Ce anomaly (Goldberg et al. 1963; Elderfield and Greaves 1982; De Baar et al. 1985, 1988). The lower MnO content and other metals like Cu, Co and Ni in the samples does not support the hydrogenous origin for Ramagiri schist belt BIF as well. During the precipitation of hydrogenous materials enrichment of various metals takes place (Piper 1974; Thomson et al. 1984). The relationship between ΣREE and the sum of $\text{Co} + \text{Cu} + \text{Ni}$ of hydrothermal and hydrogenous deposits are used by Dymek and Klein (1988) to reconstruct the fields of hydrothermal and hydrogenous deposits. The shaly BIF from Ramagiri schist belt fall far away from both the fields due to the contamination with the clastics (Fig. 13). The geochemical signatures of shaly BIF from Central block have Fe_2O_3 rich character, suggesting that precipitation of Fe did not stop during the sedimentation in an island arc related tectonic setting.

Alternatively, it can be suggested that the source of Fe, silica, REE and other trace elements may have been from bimodal volcanism, which taking place in an island arc tectonic was setting (Mishra and Rajamani 1999). It is therefore proposed that solutions circulating through mafic and felsic rocks stripped them of Fe, silica, REE and other trace elements. These elements then got mixed with the seawater and ultimately deposited as BIF. Tlig and Steinberg (1982) have reported that the finer fractions show positive Ce anomaly, related to submarine alteration of volcanic material while the coarser fractions exhibit negative Ce anomaly related to biogenic components. Similar

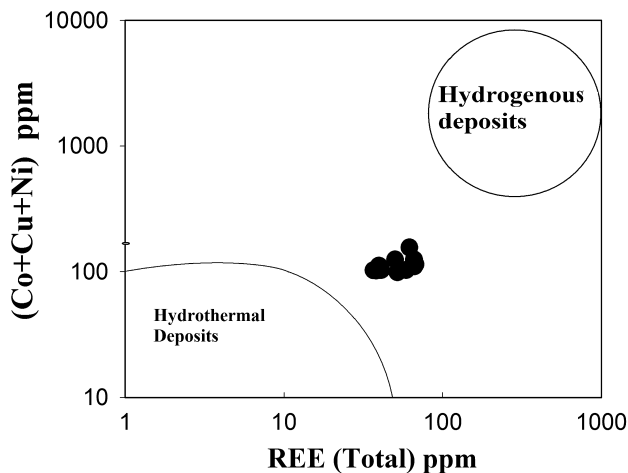


Fig. 13 Total REE versus $\text{Co} + \text{Cu} + \text{Ni}$ for shaly BIF from Ramagiri schist belt. Various fields are from Dymek and Klein (1988)

explanations have been suggested by Dymek and Klein (1988) based on their researches on BIF from 3.8 Ga Isua greenstone belt.

The shale normalized patterns for average RSB shaly BIF, Av. RSB shale are plotted with authigenic fraction of the sediments from Indian Ocean, taken a very shallow depth (Fig. 14). Modern day shallow sea sediments (authigenic component) from Indian Ocean exhibit positive Ce anomaly (Pattan et al. 2005). In the shale normalized REE patterns, the authigenic fraction from Ramagiri schist belt is represented by Av. Shaly BIF and detrital fractions (flat pattern) by Av. RSB shale (Fig. 14). The authigenic fractions of Av. shaly BIF resemble very much with that from Indian Ocean. This suggests that authigenic phases might reflect the preferred removal of LREE relative to HREE while the other phases in the ocean should be enriched in order to maintain the flat shale normalizing input. Between the MREE and HREE, the terrigenous contribution is richer in the HREE than the MREE. This suggests that there is an additional REE source other than the terrigenous input. This is supported by inference that the marine sediments with authigenic fluxes from sea water have $\text{LREE} > \text{HREE}$ (Turner and Whitfield 1979). The chemical precipitation of the chemogenic sediments can be described by mixing of detrital and authigenic components, which was probably controlled by their relative accumulation rates. The HREE enrichment might be due to the presence of minerals like chlorite, chamosite, kaolinite, Fe–oxides and oxyhydroxides as evident from XRD data in the Shaly BIF. Nesbitt (1979), Clarke Anderson (1984) and Coppin et al. (2002) have reported that certain clay minerals preferentially incorporate HREE. The elements like Si, Ti, Al, Mn, Ca, P and Zr show a good correlation with HREE. This indicates that heavy minerals like ilmenite, zircon and apatite, which could have been important phases which accommodated

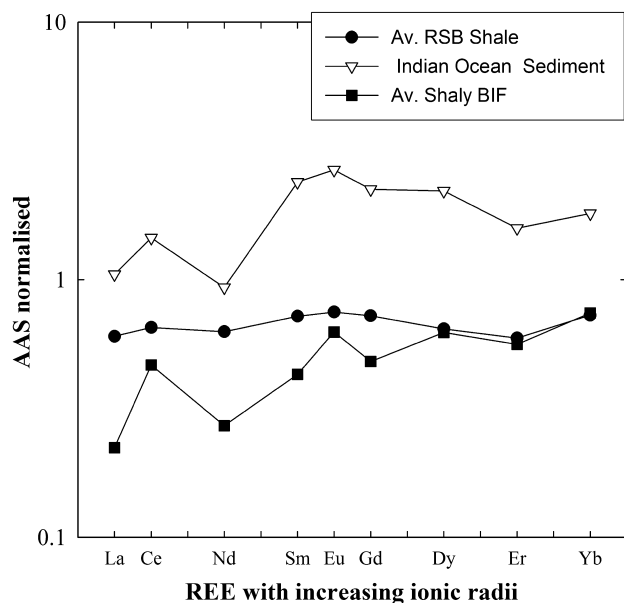


Fig. 14 Shale normalised REE patterns of the detrital and authigenic fractions of shaly BIF from Ramagiri schist belt compared with that from the authigenic fraction of sediments from Indian ocean (data from Pattan et al. 2005)

the HREEs. A good direct relationship of HREE with silica is observed. This suggests coprecipitation of mobilized HREE with secondary silica.

The understanding of REE behaviour in the anoxic waters of the modern day Cariaco Trench (De Baar et al. 1988) provides an excellent modern day analogues for the conditions that possibly prevailed in the Archean oceans. Exceptionally cerium shows a sharp increase just at or below the oxic/anoxic interface at 300 m depth. Therefore overlying oxic waters exhibit a negative Ce anomaly, whereas particulate concentration shows a complementary positive Ce anomaly. Ce anomaly in the particulates reaches maximum just above the interface, coinciding with maxima for the Fe and P. A fairly strong correlation is observed between Ce and Fe ($r = +0.6$) and Ce and P ($r = +0.33$) in the BIF from Ramagiri schist belt. This can be well explained by Fe-oxyhydroxides and phosphate precipitation at oxic/anoxic interface in the Archean oceans. The distribution of REE in the ocean water (dissolved) and particulate (suspended sediments) REE were possibly affected by oxic/anoxic interface quite similar to the modern day Cariaco Trench. It has been suggested by earlier workers that the Early Precambrian oceans were physicochemically stratified (Cloud 1973; Drever 1974; Walker et al. 1983; Holland 1973; Kasting 1987, 1993; Klein and Beukes 1993; Bau and Moller 1993; Klein and Ladeira 2000, 2002). The contemporaneous existence of a large Fe^{2+} reservoir in the deeper parts of the oceans and of shallow-water environments where iron oxyhydroxides

(oxide facies Iron Formations) precipitated points to the presence of an oxic/anoxic boundary layer in the ocean. Below this chemoline the REE distribution was controlled by input from the hydrothermal solutions whereas above it mechanisms controlling the REE distribution were probably rather similar to those operating today in the modern oceans. The presence of positive cerium anomalies and the absence of positive europium anomalies in the banded iron-formations (Klein and Beukes 1993; Derry and Jacobsen 1990) imply that iron oxidation during BIF deposition took place in waters at the surface rather than at depth (Towe 1991). The positive Ce anomaly suggests that precipitation of the chemogenic sediment took place in a weak and intermittently oxygenated environment though locally, since Archaean oceans were either anoxic or intermittently and weakly oxic (Kasting 1987, 1993; Brocks et al. 1999; Manikyamba et al. 1993; Manikyamba and Naqvi 1995; Canfield 2005). Their precipitation as insoluble ferric ion (Fe^{+3}) probably took place when ocean currents upwelling, intermittently brought them to near surface zones oxygenated by certain forms of O_2 producing bacteria thriving there (Kasting 1993). Though evidence of existence of photosynthetic bacteria has not been confirmed from Ramagiri region, but graphitic schists are present in the Central block. However, the evidences for photosynthetic generation oxygen are well preserved in the Archaean schist belts of the western and eastern Dharwar Craton such as Sandur, Chitradurga, Shimoga and Kolar (graphitic schists). They have yielded microfossils, cyanobacteria and stromatolites (Naqvi et al. 1987; Venkatachala et al. 1990; Manikyamba et al. 1993; Manikyamba and Naqvi 1995; Rao and Naqvi 1995). Cyanobacteria, the first oxygenic photosynthesizers, have been identified from organic biomarkers in sedimentary rocks as old as 2.71 Ga (Brocks et al. 1999; Canfield 2005), and may have been associated with much older microfossils and stromatolites. Thus a source of oxygen needed to precipitate FeO into Fe_2O_3 was probably photosynthetic. Whatever O_2 was available in Archaean ocean would have been produced by photosynthetic bacteria at the margin of the shallow shelf. Possibly the positive Ce anomaly in the chemogenic sediments represents the its coprecipitation with Fe^{+3} with some authigenic phase. Negative Ce anomalies in the present day sea water are the result of microbial oxidation (Moffett 1990) and in Archaean also such a process may have been responsible for the oxidation of Ce^{3+} and FeO . Takahashi et al. (2007) studied the REE distribution pattern between the bacteria and Fe oxyhydroxide in water and sediments and have observed a steep increase in HREE as compared to LREE. They have also suggested that the effect of microbial activity could potentially be extended to future researches pertaining to Banded Iron Formation.

Acknowledgments I thankfully acknowledge the financial help provided by Department of Science and Technology, New Delhi under DST Fast Track Project scheme No. HR/OY/A-16/98. Thanks are due to Prof. V. Rajamani, for allowing me to carry out geochemical analysis at Jawaharlal Nehru University, New Delhi. The critical review of the original paper by Prof. B.P. Singh, Banaras Hindu University, Varanasi has greatly helped me to improve the manuscript.

References

- Arora M, Naqvi SM (1993) Geochemistry of Archaean arenites formed by anoxic exogenic processes an example from Bababudan schist belt, India. *J Geol Soc India* 42(247):268
- Balakrishnan S, Hanson GN, Rajamani V (1999) U-Pb isotope study on zircons and sphenes from the Ramagiri area, southern India: evidence for accretionary origin of eastern Dharwar Craton during late Archean. *J Geol* 107:69–86
- Bau M (1993) Effects of syn- and post-depositional processes on the rare earth element distribution in Precambrian iron formations. *Eur J Mineral* 5:257–267
- Bau M, Dulski P (1996) Distribution of yttrium and rare-earth elements in the Penge and Kuruman iron-formations, Transvaal Supergroup, South Africa. *Precamb Res* 79:37–55
- Bau M, Moller P (1993) Rare earth element systematics of the chemically precipitated iron formations and the evolution of the terrestrial atmosphere-hydrosphere lithosphere system. *Geochim Cosmochim Acta* 57:2239–2249
- Brocks JJ, Logan GA, Buick R, Summons RE (1999) Archean molecular fossils and the early rise of eukaryotes. *Science* 285:1033–1036
- Byrne RH, Kim KH (1990) Rare earth element scavenging in seawater. *Geochim Cosmochim Acta* 54:2645–2656
- Canfield DE (2005) The early history of atmospheric oxygen. *Annu Rev Planet Sci* 33:1–36
- Chadwick B, Vasudev VN, Ahmed N (1996) The Sandur schist belt and its adjacent plutonic rocks: implications for late Archaean crustal evolution in Karnataka. *J Geol Soc India* 47:37–57
- Chakraborty KL, Majumder T (1986) Geological aspects of the banded iron formation of Bihar and Orissa. *J Geol Soc India* 28:71–91
- Clarke Anderson M (1984) Mineralogy of the rare earth elements. In: Henderson P (ed) Development in geochemistry 2—rare earth element geo-chemistry. Elsevier, Amsterdam, pp 34–60
- Cloud P (1973) Paleoenvironmental significance of the banded iron formation. *Econ Geol* 68:1135–1143
- Condie KC (1981) Archaean greenstone belts. Elsevier, Amsterdam
- Condie KC (1993) Chemical composition and evolution of the upper continental crust: contrasting results from surface amplexes and shales. *Chem Geol* 104:1–37
- Coppin F, Berger G, Bauer A, Castet S, Loubet M (2002) Sorption of Lanthanides on smectite and kaolinite. *Chem Geol* 182:57–67
- Danielson A, Möller P, Dulski P (1992) The europium anomalies in banded iron formations and the thermal history of the oceanic crust. *Chem Geol* 97:89–100
- De Baar HJW (1991) On cerium anomalies in the Sargasso Sea. *Geochim Cosmochim Acta* 55:2981–2983
- De Baar HJW, Bacon MP, Brewer PG (1985) Rare earth elements in the Pacific and Atlantic Oceans. *Geochim Cosmochim Acta* 49:1943–1959
- DeBaar HJW, German CR, Elderfield H, van Gaans P (1988) Rare earth element distributions in anoxic waters of the Cariaco trench. *Geochim Cosmochim Acta* 52:1203–1219

- Derry LA, Jacobsen SB (1990) The chemical evolution of Precambrian seawater: evidence from REEs in banded iron formations. *Geochim Cosmochim Acta* 54:2965–2977
- Devraju TC, Laajoki K (1986) Mineralogy and mineral chemistry of the manganese poor and mangniferous iron formations from the high grade metamorphic terrain of southern Karnataka, India. *J Geol Soc India* 28:134–164
- Drever JL (1974) Geochemical model for the origin of Precambrian banded iron formations. *Geol Soc Am Bull* 85:1099–1106
- Dutta RK, Acharya R, Nair GCA, Chintalapudi SN, Chakravorty V, Reddy AVR, Manohar SB (2005) Application of k0-based INAA method in the studies of rare earth and other elements in manganese nodules from Indian ocean. *J Nucl Radiochem Sci* 6:139–143
- Dymek RF, Klein C (1988) Chemistry, petrology and origin of banded iron formation lithologies from the 3800 Ma Isua supracrustal belt, West Greenland. *Precamb Res* 39:247–302
- Elderfield H, Greaves MJ (1982) The rare earth elements in seawater. *Nature* 296:214–219
- Elderfield H, Hawkesworth CJ, Greaves MJ, Calvert SE (1981) Rare earth element geochemistry of oceanic ferromanganese nodules and associated sediments. *Geochim Cosmochim Acta* 45:513–528
- Eugester HP, Chou IM (1973) Depositional environments of Precambrian banded iron formations. *Econ Geol* 68:1144–1168
- Ewers WE, Morris RC (1981) Studies on the Dales Gorge member of the Brockman Iron formation. Western Australia. *Econ Geol* 77:1929–1953
- Fryer BJ (1977) Rare earth evidence in iron formations for changing Precambrian oxidation states. *Geochim Cosmochim Acta* 41:361–367
- Fryer BJ (1983) Rare earth elements in iron formations. In: Trendall AF, Morris RC (eds) *Iron formation: facts and problems*. Elsevier, Amsterdam, p 358
- Fryer BJ, Fyfe WS, Kerrich R (1979) Archaean volcanogenic oceans. *Chem Geol* 24:25–33
- Garrels RM, Perry EA Jr, Mackenzie FT (1973) Genesis of Precambrian iron-formations and the development of atmospheric oxygen. *Econ Geol* 68:1173–1179
- German CR, Elderfield H (1990) Application of the Ce anomaly as a paleoredox indicator: the ground rules. *Paleoceanography* 5: 823–833
- German CR, Holliday BP, Elderfield H (1991) Redox cycling of rare earth elements in the suboxic zone of the Black Sea. *Geochim Cosmochim Acta* 55:3553–3558
- Giritharan TS, Rajamani V (1998) Geochemistry of the metavolcanics of the Hutt-Maski schist belt, south India: implications to gold metallogeny in the eastern Dharwar Craton. *J Geol Soc India* 51:583–594
- Goldberg ED, Koide M, Schmitt RA, Smith RH (1963) Rare earth distributions in the marine environment. *J Geophys Res* 68:4209–4217
- Goldstein SJ, Jacobsen SB (1988) Rare earth elements in river waters. *Earth Planet Sci Lett* 89:35–47
- Goodwin AM (1991) Precambrian geology. Academic Press, New York, p 666
- Goodwin AM, Thode HG, Chau CL, Karkhanis SN (1985) Chemostratigraphy and origin of the late Archaean siderite-pyrite rich Helen Iron Formation, Michipicoten belt. *Can J Earth Sci* 22:72–84
- Gross GA (1980) A classification of iron formations based on depositional environments. *Can Mineral* 18:215–222
- Gross GA (1991) Genetic concepts for iron-formation and associated metalliferous sediments. *Econ Geol Monogr* 8:51–88
- Holland DH (1973) The oceans: a possible source of iron in iron formations. *Econ Geol* 68:1169–1172
- Jacobsen SB, Pimental-Klose MR (1988) A Nd isotopic study of the Hamersley and Michipicoten banded iron formations: the source of REE and Fe in Archaean oceans. *Earth Planet Sci Lett* 87:29–44
- Kasting JF (1987) Theoretical constraints on oxygen and carbon-dioxide concentrations in the Precambrian atmosphere. *Precamb Res* 24:205–229
- Kasting JF (1993) Earth's early atmosphere. *Science* 259:920–926
- Khan RMK, Naqvi SM (1996) Geology, geochemistry and genesis of BIF of Kushtagi Schist Belt, Archaean Dharwar Craton, India. *Mineral Deposita* 31:123–133
- Khan RMK, Govil PK, Naqvi SM (1992) Geochemistry and genesis of banded iron formation from Kudremukh schist belt, Karnataka nucleus, India. *J Geol Soc Ind* 40:311–328
- Klein C, Beukes NJ (1993) Sedimentology and geochemistry of the glaciogenic late Proterozoic Raptian iron-formation in Canada. *Econ Geol* 88:542–565
- Klein C, Ladeira AE (2000) Geochemistry and petrology of some proterozoic banded iron-formations of the Quadrilátero Ferrífero, Minas Gerais, Brazil. *Econ Geol* 95:405–428
- Klein C, Ladeira AE (2002) Petrography and geochemistry of the least altered banded iron-formation of the Archean Carajás formation, Northern Brazil. *Econ Geol* 97:643–651
- Knoll AH (2003) The geological consequences of evolution. *Geobiology* 1:3–14
- LaBerge GL (1988) Possible biological origin of Precambrian iron-formations. *Econ Geol* 68:1098–1109
- Liu YG, Schmitt RA (1990) Cerium anomalies in western Indian Ocean Cenozoic carbonates, Leg 115. *Proc Ocean Drilling Program Sci Res* 115:709–714
- Liu YG, Miah MRU, Schmitt RA (1988) Cerium, a chemical tracer for paleo-oceanic redox conditions. *Geochim Cosmochim Acta* 5:1361–1371
- McLeod KG, Irving AJ (1996) Correlation of cerium anomalies with indicators of paleoenvironment. *J Sediment Res* 66(5):948–955
- Majumder T, Whitley JE, Chakraborty KL (1984) Rare earth elements in the Indian banded iron formation. *Chem Geol* 45(3):203–211
- Manikyamba C, Naqvi SM (1995) Geochemistry of Fe–Mn formations of the Archaean Sandur schist belt, India—mixing of clastic and chemical processes at a shallow shelf. *Precamb Res* 72:69–95
- Manikyamba C, Balaram V, Naqvi SM (1993) Geochemical signatures of polygenetic origin of a banded iron formation (BIF) of the Archaean Sandur greenstone belt (Schist belt), Karnataka nucleus, India. *Precamb Res* 61:137–164
- Manikyamba C, Naqvi SM, Moeen S, Gnaneshwar Rao T, Balram V, Ramesh SL, Reddy GLN (1997) Compositional heterogenetics of greywackes from late Archaean Sandur belt: implications for active plate margin processes. *Precamb Res* 84:117–138
- Marchig V, Gundlach H, Moller P, Schley F (1982) Some geochemical indicators for discrimination between diagenetic and hydrothermal metalliferous sediments. *Marine Geol* 50:241–256
- McLennan SB (1989) Rare earth elements in sedimentary rocks. Influence of provenance and sedimentary processes. In: Lipin BR, McKay GA (Eds.) *Geochemistry and mineralogy of the rare earth elements*. Miner Soc Am, Washington, pp. 169–200
- Michard A, Albererde F (1986) The REE content of some hydrothermal fluids. *Chem Geol* 55:51–60
- Michard A, Michard G, Stoben D, Stoffers P, Cheminee JL, Binard N (1993) Submarine thermal springs associated with young volcanoes: the Teahitia Vents, Society Islands, Pacific Ocean. *Geochim Cosmochim Acta* 57:4977–4986
- Middelburg JJ, Weijden CHVD, Woittiez JRW (1988) Chemical processes affecting the mobility of major, minor and trace elements during weathering of granitic rocks. *Chem Geol* 68:253–273

- Miller RG, O’Nions RK (1985) Sources of Precambrian chemical and clastic sediments. *Nature* 314:325–330
- Mishra Meenal, Rajamani V (1999) Significance of the Archaean bimodal volcanics from the Ramagiri schist belt in the formation of eastern Dharwar Craton. *J Geol Soc India* 54:563–583
- Mishra Meenal, Rajamani V (2003) Geochemistry of the Archaean Metasedimentary rocks from the Ramagiri Schist Belt, Eastern Dharwar Craton, India: implications to Crustal evolution. *J Geol Soc India* 62:717–738
- Moffett JW (1990) Microbially mediated cerium oxidation in sea water. *Nature* 345:421–423
- Naqvi SM, Venkatachala BS, Shukla Manoj, Kumar B, Natarajan R, Sharma Mukund (1987) Silicified cyanobacteria from the cherts of Archaean Sandur schist belt, Karnataka, India. *J Geol Soc India* 29:535–539
- Nealson KH, Myers CR (1990) Iron reduction by bacteria: a potential role in the genesis of banded iron formation. *Am J Sci* 290A:35–45
- Nesbitt HW (1979) Mobility and fractionation of rare earth elements during weathering of a granodiorite. *Nature* 279:206–210
- Pattan NJ, Pearce NJG, Mislankar PG (2005) Constraints in using Cerium-anomaly of bulk sediments as an indicator of paleo bottom water redox environment: a case study from the Central Indian Ocean Basin. *Chem Geol* 221:260–278
- Piedgras DJ, Wasserburg GJ, Dasch EJ (1979) Strontium and Neodymium isotopes in the hot springs on the East Pacific Rise and Guayamas Basin. *Earth Planet Sci Lett* 45:223–236
- Piper DZ (1974) Rare earth elements in ferromanganese nodules and other marine phases. *Geochim Cosmochim Acta* 38:1007–1022
- Rao TG (1992) Geochemistry and genesis of Banded Iron Formation (BIF) from the Central part of the Chitradurga schist belt, Karnataka. Ph.D. Thesis, Osmania University, Hyderabad, p 350
- Rao TG, Naqvi SM (1995) Geochemistry, depositional environment and tectonic setting of the BIF’s of the Late Archaean Chitradurga Schist Belt, India. *Chem Geol* 121:217–243
- Rosing MT, Frei R (2004) U-rich Archaean sea floor sediments from Greenland: indication of 3700 Ma oxygenic photosynthesis. *Earth Planet Sci Lett* 217:237–244
- Ruhlin DE, Owen RM (1986) The rare earth element geochemistry of hydrothermal sediments from the East Pacific Rise: examination of a sea water scavenging mechanism. *Geochim Cosmochim Acta* 49:2545–2560
- Shapiro L, Brannock WW (1962) Rapid analyses of silicate, carbonate and phosphate rocks. *US Geol Surv Bull* 48:49–55
- Shimizu H, Umemoto N, Masuda A, Appel PWU (1990) Sources of iron-formations in the Archaean Isua and Malene supracrustals, West Greenland: evidence from La–Ce and Sm–Nd isotopic data and REE abundances. *Geochim Cosmochim Acta* 54:1147–1154
- Sholkovitz ER (1988) Rare earth elements in the sediments of the North Atlantic Ocean, Amazon delta, and East China Sea: reinterpretation of terrigenous input patterns to the oceans. *Am J Sci* 288:236–281
- Sholkovitz ER, Schneider DL (1991) Cerium redox cycles and rare earth elements in the Sargasso Sea. *Geochim Cosmochim Acta* 55:2737–2743
- Siddaiah NS, Hanson GN, Rajamani V (1994) Rare Earth Element evidence for syngenetic origin of an Archaean stratiform Gold sulfide deposit, Kolar schist belt, South India. *Econ Geol* 89:1152–1166
- Sun S-S, McDonough WF (1989) Chemical and isotopic systematics of oceanic basalts: implications for mantle composition and processes. In: Saunders AD, Norry MJ (eds) *Magmatism in the ocean basins*. Geol. Soc Sp. Publ., London, pp 313–345
- Takahashi Y, Hirata T, Shimizu H, Ozaki T, Fortin D (2007) A rare earth element signature of bacteria in natural waters? *Chem Geol* 244:569–583
- Taylor SR, McLennan SM (1985) The continental crust: its composition and evolution. Blackwell, Oxford, p 311
- Thomson J, Carpenter MSN, Colley S, Wilson TRS, Elderfield H, Kennedy H (1984) Metal accumulation rates in northwest Atlantic pelagic sediments. *Geochim Cosmochim Acta* 48:1935–1948
- Tlig S, Steinberg M (1982) Distribution of rare earth elements (REE) in size fractions of recent sediments of the Indian Ocean. *Chem Geol* 37:317–333
- Towe KM (1991) Aerobic carbon cycling and cerium oxidation: significance for Archean oxygen levels and banded iron-formation deposition. *Glob Planet Change* 5(1–2):113–123
- Trendall AF, Morris RC (eds) (1983) *Iron formation: facts and problems*. Elsevier, Amsterdam, p 558
- Turner DR, Whitfield M (1979) Control of seawater composition. *Nature* 281:468–469
- Venkatachala BS, Shukla M, Sharma M, Naqvi SM, Srinivasan R, Uday Raj B (1990) Archaean microbiota from the Donimalai formation, Dharwar Supergroup, India. *Precamb Res* 47:27–34
- Walker JCG, Klein C, Schidlowski M, Schopf JW, Stevenson DJ, Walter MR (1983) Environmental evolution of the Archaean–early proterozoic earth. In: Schopf JW (ed) *Earth’s earliest biosphere: its origin and evolution*. Princeton Univ. Press, Princeton, pp 260–290
- Wilde P et al (1996) The whole-rock cerium anomaly: a potential indicator of eustatic sea-level changes in shales of the anoxic facies. *Sediment Geol* 101:43–53
- Zachariah JK, Hanson GN, Rajamani V (1995) Post crystallization disturbances in the Nd and Pb Isotope systematics of metabasalts from the Ramagiri Schist Belt, south India. *Geochim Cosmochim Acta* 59:3189–3203
- Zachariah JK, Mohanta MK, Rajamani V (1996) Accretionary evolution of the Ramagiri schist belt, eastern Dharwar Craton. *J Geol Soc India* 47:279–291
- Zachariah JK, Rajamani V, Hanson GN (1997) Geochemistry of metabasalts from the Ramagiri schist belt, south India: petrogenesis, source characteristics and implications to the origin of the eastern Dharwar Craton. *Contrib Mineral Petrol* 129:87–104